Effects of the Cellular Morphology on Fatigue Deformation Mechanisms of Physically Foamed Polycarbonate

Kübra Güzel, Jan-Christoph Zarges, and Hans-Peter Heim*
Institute of Materials Engineering – Polymer Technology (IfW), University of Kassel

Abstract

In this study, the tension–tension fatigue behavior of foam injection molded thermoplastic microcellular Polycarbonate (PC) is characterized. The variation in morphology is obtained by modifying the mold temperature, injection volume, injection flow rate, and blowing agent content (physical and chemical) in the polymer melt. The relationship between the wide range of morphological qualities and relevant fatigue properties is made explicit via a statistical correlation coefficient analyses. The analysis is made between the fatigue life, cumulative dissipated energy, strain energy, damping and dynamic modulus including the effects of morphology such as cell diameters, distance between cells, cell density, density reduction, homogeneity of cell size distribution, sphericity of cells and cell volume. Additionally, the pattern recognition of different cellular morphologies is made via hierarchical clustering analysis. As a result, the distinct cell morphologies subjected to sinusoidal cyclic-dynamic as well as quasi-static tensile load to determine the fracture behavior as a function of the morphological appearances.

Introduction

In 21st century, energy became one of the main influencing factor of the economy with the increase in population and consumption [1]. The high cost of oil and gas sources, in addition to the concerns about global warming caused by excessive carbon dioxide emissions from industry, are leading to increased interest in lightweight construction, which is bringing their processing technology into focus. In this context, the optimization of the process-morphology-property relationship to reduce material requirements and component weight while simultaneously optimizing mechanical properties is one of the main topics of interest. Since the mechanical properties of the foamed structures are sensitive to microstructural details, the design of the part should be adapted to these properties to avoid premature failure. Therefore, the resulting foam morphology is varied not only by the injection molding parameters, but also by a special core back molding technique, the so-called *pull-and-foam method*, which has been explained in previous studies [2–7]. Güzel et al. (2021) made a quantitative study on the indicators of cell morphology and the resulting flexural properties using a statistical model. The injection processing parameters, such as mold temperature, blowing agent concentration, and volume flow rate, are varied to achieve variation in morphological properties (cell size, distance between cells, cell density, and compact skin layer thickness). Based on morphological analyses and the results of bending tests, correlations are determined between structural and flexural properties. The results showed that cell distance, homogeneity, sphericity, and cell density are found to be the best explanatory variables to explain the change in flexural strength. It was also found that a higher stress is required for the propagation of a crack with a larger cell structure and a greater distance to adjacent cells [5]. In the following study made by Güzel et al. (2023), the deformation behavior of microcellular polycarbonate was investigated depending on distinctive morphological patterns technique during uniaxial quasi-static tensile loading with 3D Digital Image Correlation. The full-field strain histories of each morphology patterns illustrate multiple localized high-strain field beyond the yield point. This is because heterogeneity in cell size distribution, as well as spacing between cells, leads to differences in morphology and ultimately differences in stress concentration around subregions of the cellular material. Thus, heterogeneity in foam morphology leads to differential elongation of cell walls, with larger cells elongating while smaller cells limit elongation, resulting in more pronounced local deformation [7].

On the one hand, many studies have been conducted to characterize the quasi-static mechanical deformation behavior of cellular materials, tensile properties [5,7–11], compressive strength [12–14] and flexural properties [6,15–17]. On the other hand, there is not much information in the open literature about the fatigue of microcellular thermoplastics. Seeler and Kumar conducted the preliminary study on the fatigue behavior of microcellular polycarbonate in 1993. It was found that the fatigue life of microcellular polycarbonate with a relative density of 0.97 is higher than that of compact polycarbonate [11,18]. Dynamical fatigue deformation behavior of PVC foams [13,14,19–22] and epoxy resin foams [23,24] are also studied to certain extend. However, considerable efforts are still required to establish the correlation between the distinct cell morphological properties and fatigue properties as well as crack initiation and propagation in the context of the common morphology patterns.

In this study, different foam injection molding processing parameters are used to create a variance in cell morphology and modify the geometric appearance of the cell structure. Empirical cyclic-dynamic tensile tests are carried out to establish correlation between the influencing morphological parameters and the fatigue life, dynamic modulus, accumulated dissipated energy as well as strain energy. Consequently, the distinct cell morphologies subjected to imposed sinusoidal cyclic-dynamic loading as well as quasi-static tensile loading are investigated to determine the fracture behavior as a function of the morphological appearances.

Materials and Methods

Pure polycarbonate (Makrolon® 2405) with a melt volume rate (MVR) of 19 cm^3/10 min (300 ◦C 1,2 kg) and a density (ρ) of 1.20 g/cm^3 was provided from Covestro AG (Leverkusen, Germany).

In order to produce test specimens, an all-hydraulic injection molding machine Arburg Allrounder 470S (Arburg GmbH + Co KG, Loßburg, Germany) equipped with a core-back insert was used. Precise amount (0.2, 0.4 and 0.8 wt%) of supercritical nitrogen (N_2) was injected into the molten polymer by using the MuCell® technology (Trexel, Inc., Woburn, Massachusetts). A chemical blowing agent (cba) of 0.5 wt% (TRACEL® IM 4221, Tramaco, Tornesch, Germany) was mixed into the polymer as a nucleation agent to create the morphology. Initially, the mold cavity was set as a rectangular plate with a size of 120 mm x 80 mm and a thickness of 3 mm. With the help of an expandable core-back system, four highly foamed rectangular ribs of different widths (4/6/8/10 mm) extended from 0.5 to 8.5 mm. Detailed information on the variation of injection molding process parameters corresponding to defined morphology pattern is given in Table 1.

Table 1. Injection molding processing parameters

Morph. Patterns	Mold Temp.	Injection Flow Rate	Blowing Agent Content	Injection Volume	Melt Temp.
	[°C]	[cm^3/s]	[wt%]	[cm^3]	[°C]
Morph_1	30	50	0.4	45	290
Mroph_2	80	150	0.4	50	290
Mroph_3	80	150	0.4 and 0.5(cba)*	55	290
Morph_4	50	165	0.2	55	280
Morph_5	40	160	0.4	55	280
Morph_6	40	50	0.4	45	280
Morph_7	30	100	0.6	55	280
Morph_8	30	150	0.2	50	290
Morph_9	80	150	0.2	50	290

* Abbreviation for the chemical blowing agent

Mechanical Characterization

The 10 mm width extended rib was concentrically milled out of the produced specimens by a Computerized Numerical Control (CNC) machine (DMO 100 Monoblock, Deckel Maho, Bielefeld, Germany) in order to characterize the deformation behavior of thermoplastic closed-cell cellular structure without the compact surface skin layer. Quasi-static tensile test was carried out by a universal testing machine (Z010, Zwick Roell, Ulm, Germany) with a constant crosshead speed of 2 mm/min at standard room temperature and relative humidity (23 °C, 50 %). The dimension of the test specimen is illustrated in a previous study [7]. Uniaxial fatigue experiments were conducted using an MTS 810 servo-hydraulic pulser with a load cell of 25 kN and the extensometer with 25 mm of gage length (MTS) during the stress controlled tests. The specimens were tested using a sinusoidal load with a load ratio of 0.2 and a testing frequency of 10 Hz. The variation in maximal stress (5, 10, 12, 15, 20 MPa) was made to determine the influence of the mean stress on the Wöhler curve.

Morphology Characterization

Geometric aspects of the cell structure were identified using a digital light microscope (Keyence VHX-7000, Keyence, Ōsaka, Japan) with a 50X magnification. Therefore, measurement area with a length of 30 mm was cut and prepared out in the center of tensile test specimen. The obtained digital images were subjected to image processing software (ImageJ) to calculate cell size distribution, cell diameter (median) and distance between cells (average). Additionally, the cell density (N), the number of cells formed per unit volume (cm^3) was determined using Eq. (1) as following [2].

$$N = \left(\frac{n}{A}\right)^{3/2} x \quad \left(\frac{1}{1-v_f}\right) \tag{1}$$

$$v_f = \quad 1 - \frac{\rho_{foam}}{\rho_{solid}} \tag{2}$$

Where n denotes the number of cells counted in the measurement area (A) of the microscopic image, V_f is the local void fraction and ρ_s and ρ_f indicate, respectively, the density of solid and foam material.

Three-dimensional indicators of the cellular morphology such as sphericity and cell volume were determined using X-ray microtomography (μCT) Zeiss XRadia 520 Versa microscope (Zeiss, Oberkochen, Germany). Sphericity indicates the degree of the anisotropy in the morphology. Hereat, a sphericity of 1 represents a perfect roundness. In this case, the anisotropic aspect ratio (R) used as sphericity that is the ratio of cell height (h) (in the rising direction) to the cell width (l) (in the transverse direction). Homogeneity is the indicator of the

uniformity of the cell size distribution, which is calculated using the novel method "Cell Distribution Index (CDI)"[5,25] A value of 1 is a sign of monodispersion and the differentness in cell size causes an increase in CDI.

$$CDI = \frac{\Phi_{\mathrm{D}}}{\Phi_{\mathrm{N}}} \tag{3}$$

$$\Phi_N = \frac{\sum_{\mathrm{i}} N_i \Phi_i}{\sum_{\mathrm{i}} N_i} \tag{4}$$

$$\Phi_D = \frac{\sum_{\mathrm{i}} N_i \Phi_i^2}{\sum_{\mathrm{i}} N_i \Phi_i} \tag{5}$$

Where (Φ_{i}) and (N_{i}) denote the diameter of cells in microns and the number of the cells having diameter Φ_{i}.

Results and Discussion

Figure 1 illustrates the influence of the morphological properties (cell dameter, cell distance, density reduction, cell density, sphericity and homogenetiy) on dynamic modulus (E_{dyn}), damping (D), number of cycles (N), total strain energy at the fatigue (W^{S}), total dissipated energy at the fatigue (W^{D}), accumulated dissipated energy ($\sum W^{\mathrm{D}}$). It was found out that there is no strong relationship between number of cycles and morphological properties, but only present a positive moderate correlation with density reduction and cell distance. The predictability are R^2- value=0.43 and 0.49, respectively. Strain energy on the other hand shows a strong reverse parabolic relationship with the cell density (R^2-value =0.79). The dynamic modulus is also affected by the cell density and shows a strong parabolic, however, is not an inverse relationship (R^2-value=0.72). Considering the curve trends, it can be concluded that strain energy is dominating the dynamic modulus, which is attributed to the fact that foam material behaving more elastic behavior during the fatigue test [26]. Moreover, the change in density reduction has a high strong effect on the dynamic modulus, which gives the highest correlation coefficient in the overall correlation matrix (R^2- value=0.80). A further increase in average cell distance results in decreasing accumulated dissipated energy (R^2-value =0.76). The rate of decrease is high at first and continues to be relatively constant after a certain increase in cell distance. It can be concluded that the energy transfer to the atmosphere is lower at the beginning when the distance between the cells is smaller, owing to the better thermal conductivity of the cell structure [27]. As a result, a rise in temperature is observed in the overall test specimen. At maximum load, the cells are irreversibly elongated in the loading direction and restrain the polymer matrix to return to its lower strained position, resulting in a multiaxial stress state and reducing the mobility of the molecules. Therefore, an increase in cell density compared to a larger cell distance has a positive effect on energy dissipation to a certain extent.

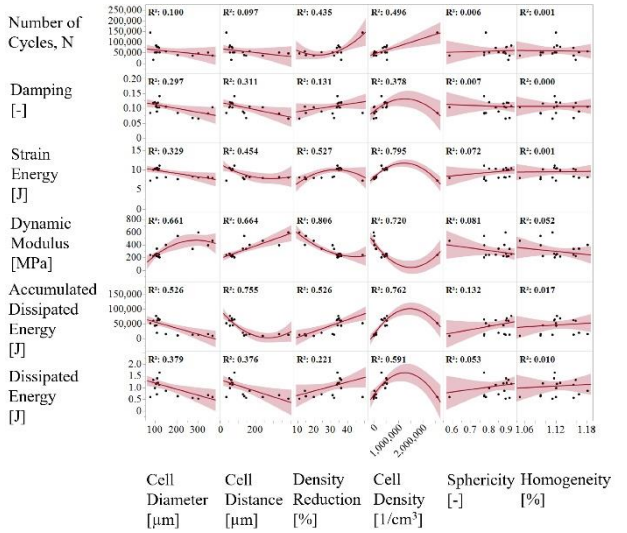

Figure 1. Illustration of the influence of morphological properties on dynamical of foamed polycarbonate.

When it comes to the Figure 2, nine (9) different cellular morphologies of polycarbonate are illustrated with a representative microscopic image after the image processing by applying the "threshold" that separates the cells of interest (colored black) from the compact material (colored white). It is visible that compact material achieves the maximum material stiffness.

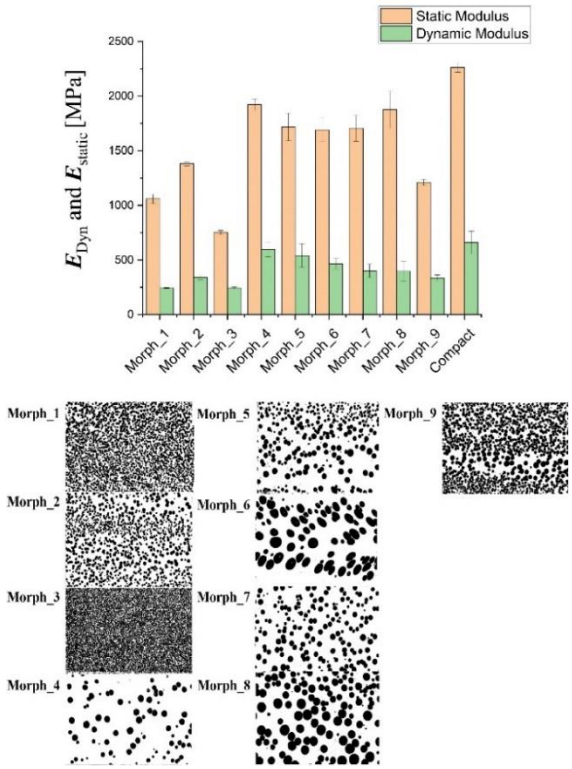

Figure 2. Dynamic and elastic modulus as a faction of different morphology patterns

However, *Morph_4* displays a small difference in dynamic modulus compared to the compact material despite the reduction in static modulus. This can be attributed to the fact when the cell distance/cell diameter is ≥ 1.3, the polymer chains have high mobility due to the low degree of elongation in the cell walls leading to stiffer material[28].

Figure 3 shows the fatigue life as a function of applied maximum stress. It is noticeable that below 20 MPa applied stress, under the same frequencies, the fatigue life expectancy varies due to the changes in the overall morphology. *Morph_1*, *Moprh_2* and *Morph_3* exhibited longer fatigue life, in contrast to the larger cell diameter as well as high density morphologies between 15 and 10 MPa maximum stress. As it is seen in Figure 1 accumulated energy dissipation capacity increase with a decrease in cell diameter and an incrase in the density reduction resulting in a longer fatigue life.

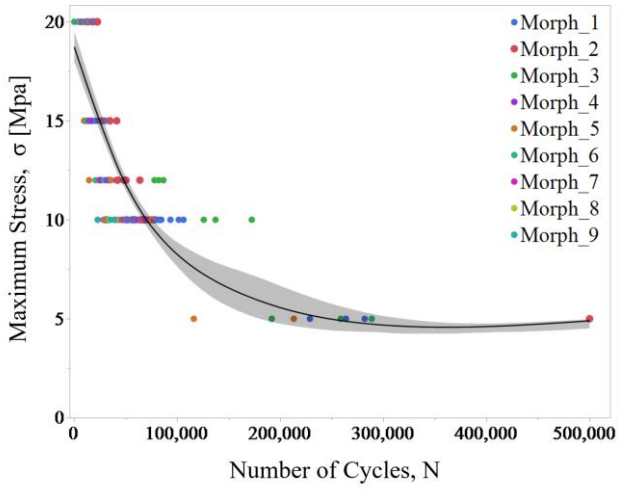

Figure 3. Polycarbonate experimental maximum stress-life fatigue behavior for a frequency of 10 Hz at room temperature

Figure 4 illustrates the accumulative dissipated energy as a function of applied maximum stress for *Morph 3* and *Morph 6*. On the one hand, *Morph 6* displays a linear decrease with the increase of applied maximum stress. A higher maximum stress means a higher minimum stress. Therefore, the samples are subjected to greater loads, resulting a decrease in life cycles and reducing energy absorption capacity. On the other hand, *Morph_3* shows a different tendency. High cell density, smaller cell distance as well as smaller cells diameters have a strong positive effect on the energy absorbance capacity at lower loads. Hereat, maximum stress of 10MPa, the morphology reaches the maximum accumulated energy dissipitation, which is 75,158.65 J, while *Morph_6* reaches 13,512.83 J at maximum. The compact material shows in average 18,898.49 J energy dissipation at the same applied mean stress.

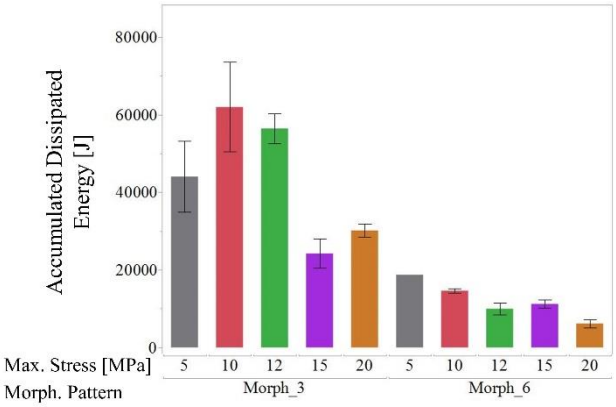

Figure 4. The illustration of the accumulated dissipated energy depending upon applied max stress (n ≥2, Morph_6 was tested only once with 5 MPa maximum stress)

Conclusions

In this study, a statistical analysis of correlation is measured by a correlation coefficients between the distinctive cell morphology properties and cyclic-dynamic tensile properties. Moreover, the common thermoplastic foam morphologies are examined under the cyclic-dynamic tension-tension fatigue test to understand the influence of the overall morphology appearances and resulting corresponding fatigue life, accumulated dissipated energy and dynamic modulus of each morphology pattern. The results show that an increase in average cell distance results in decreasing accumulated dissipated energy (R^2- value =0.76). The rate of decrease is initially high and remains relatively constant after a certain increase in cell distance. It was concluded that enhanced cell density with smaller distance between cells improves energy absorption capacity. Moreover, *Morph_4* exhibits a small difference in dynamic modulus compared to compact material, with the cell distance to cell diameter ratio close to 1.3, which allows the polymer chains to be highly mobilized due to the low elongation of the cell walls. The maximum stress and fatigue life plot showed that morphologies with a high density reduction and a smaller diameter but high number of cells resulted in a longer fatigue life between 15 and 10 MPa maximum stress. This hypothesis was also found to be present in the measurement of the accumulated dissipation energy of two completely different morphologies (*Morph_3* and *Morph_6*) with different maximum stresses. High cell density, smaller cell distance and cell diameter provide an average of 5.5 times higher energy absorption, leading to longer life at a maximum load of 10 MPa.

Acknowledgements

This research was funded by Deutsche Forschungsgemeinschaft (DFG), (Grant No 411667746).

References

[1] Energy in the 21st century, (n.d.). https://pubsapp.acs.org/subscribe/archive/ci/31/i01/html/01chen.html (accessed August 22, 2023).

[2] M. Tromm, V. Shaayegan, C. Wang, H.-P. Heim, C.B. Park, Investigation of the mold-filling phenomenon in high-pressure foam injection molding and its effects on the cellular structure in expanded foams, Polymer. 160 (2019) 43–52. https://doi.org/10.1016/j.polymer.2018.11.006.

[3] H.-P. Heim, M. Tromm, General aspects of foam injection molding using local precision mold opening technology, Polymer. 56 (2015) 111–118. https://doi.org/10.1016/j.polymer.2014.10.070.

[4] H.-P. Heim, M. Tromm, Formation of morphology as a function of process control by foam injection molding of a functionally graded component, (2014). https://doi.org/10.17170/kobra-202206246399.

[5] K. Güzel, H.-P. Heim, The Effect of Injection Molding Parameters on Microcellular Foam Morphology, (2021). https://doi.org/10.17170/kobra-202206216374.

[6] K. Güzel, J.-C. Zarges, H.-P. Heim, Effect of Cell Morphology on Flexural Behavior of Injection-Molded Microcellular Polycarbonate, Materials. 15 (2022) 3634. https://doi.org/10.3390/ma15103634.

[7] K. Güzel, J.-C. Zarges, H.-P. Heim, In-situ full-field deformation analysis of injection-molded microcellular polycarbonate according to foam morphology patterns, Polymer Testing. 124 (2023) 108102. https://doi.org/10.1016/j.polymertesting.2023.108102.

[8] Md.E. Kabir, M.C. Saha, S. Jeelani, Tensile and fracture behavior of polymer foams, Materials Science and Engineering: A. 429 (2006) 225–235. https://doi.org/10.1016/j.msea.2006.05.133.

[9] J. Hou, G. Zhao, G. Wang, G. Dong, J. Xu, A novel gas-assisted microcellular injection molding method for preparing lightweight foams with superior surface appearance and enhanced mechanical performance, Materials & Design. 127 (2017) 115–125. https://doi.org/10.1016/j.matdes.2017.04.073.

[10] F. Ramsteiner, N. Fell, S. Forster, Testing the deformation behaviour of polymer foams, Polymer Testing. 20 (2001) 661–670. https://doi.org/10.1016/S0142-9418(00)00090-8.

[11] K.A. Seeler, V. Kumar, Tension-Tension Fatigue of Microcellular Polycarbonate: Initial Results, Journal of Reinforced Plastics and Composites. 12 (1993) 359–376. https://doi.org/10.1177/073168449301200308.

[12] S. Zhang, J.M. Dulieu-Barton, R.K. Fruehmann, O.T. Thomsen, A Methodology for Obtaining Material Properties of Polymeric Foam at Elevated Temperatures, Experimental Mechanics. 52 (2011) 3.

[13] H. Yao, Y. Pang, X. Liu, J. Qu, Experimental Study of the Dynamic and Static Compression Mechanical Properties of Closed-Cell PVC Foams, Polymers. 14 (2022) 3522. https://doi.org/10.3390/polym14173522.

[14] I.M. Daniel, J.-M. Cho, Characterization of Anisotropic Polymeric Foam Under Static and Dynamic Loading, Exp Mech. 51 (2011) 1395–1403. https://doi.org/10.1007/s11340-011-9466-3.

[15] H.-P. Heim, M. Tromm, Injection molded components with functionally graded foam structures – Procedure and essential results, Journal of Cellular Plastics. 52 (2016) 299–319. https://doi.org/10.1177/0021955X15570077.

[16] L. Marsavina, T. Sadowski, M. Kneć, R. Negru, Non-linear behaviour of foams under static and impact three point bending, International Journal of Non-Linear Mechanics. 45 (2010) 969–975. https://doi.org/10.1016/j.ijnonlinmec.2010.03.007.

[17] K.S. Yen, M.M. Ratnam, H.M. Akil, Measurement of flexural modulus of polymeric foam with improved accuracy using moiré method, Polymer Testing. 29 (2010) 358–368. https://doi.org/10.1016/j.polymertesting.2009.12.011.

[18] V. Kumar, J.E. Weller, A model for the unfoamed skin on microcellular foams, Polym. Eng. Sci. 34 (1994) 169–173. https://doi.org/10.1002/pen.760340302.

[19] K. Kanny, H. Mahfuz, T. Thomas, S. Jeelani, Static and Dynamic Characterization of Polymer Foams Under Shear Loads, Journal of Composite Materials. 38 (2004) 629–639. https://doi.org/10.1177/0021998304042390.

[20] D. Zenkert, A. Shipsha, M. Burman, Fatigue of Closed Cell Foams, Jnl of Sandwich Structures & Materials. 8 (2006) 517–538. https://doi.org/10.1177/1099636206065886.

[21] M. Burman, D. Zenkert, Fatigue of foam core sandwich beams—1: undamaged specimens, International Journal of Fatigue. 19 (1997) 551–561. https://doi.org/10.1016/S0142-1123(97)00069-8.

[22] M. Burman, D. Zenkert, Fatigue of foam core sandwich beams—2: effect of initial damage, International Journal of Fatigue. 19 (1997) 563–578. https://doi.org/10.1016/S0142-1123(97)00068-6.

[23] K. Kurek, A.K. Bledzki, Fatigue Behavior of Composites with Foamed Matrix, Journal of Reinforced Plastics and Composites. 13 (1994) 1116–1134. https://doi.org/10.1177/073168449401301204.

[24] A.K. Bledzki,, J. Gassan, The Accumulated Dissipated Energy of Composites Under Fatigue Loadings, Science and Engineering of Composite Materials. 8 (1999) 99–106. https://doi.org/10.1515/SECM.1999.8.2.99.

[25] S. Rizvi, M. Alaei, A. Yadav, N. Bhatnagar, Quantitative analysis of cell distribution in injection molded microcellular foam, Journal of Cellular Plastics. 50 (2014) 199–219. https://doi.org/10.1177/0021955X14524081.

[26] M. Berer, D. Tscharnuter, G. Pinter, Dynamic mechanical response of polyetheretherketone (PEEK) exposed to cyclic loads in the high stress tensile regime, International Journal of Fatigue. 80 (2015) 397–405. https://doi.org/10.1016/j.ijfatigue.2015.06.026.

[27] S. Kang, J.Y. Choi, S. Choi, Mechanism of Heat Transfer through Porous Media of Inorganic Intumescent Coating in Cone Calorimeter Testing, Polymers. 11 (2019) 221. https://doi.org/10.3390/polym11020221.

[28] M. Rohledar, Dynamisches Lastverhalten von mikrozellularen Polycarbonatschäumen, Morphologie, Energieabsorption und Temperatureinfluss, Dissertation, Universität Kassel, 2015.